The spin Hall effect in single-crystalline gold thin films*

Dai Tian(田岱)[1,2], Caigan Chen(陈才干)[1,2], Hua Wang(王华)[1,2], and Xiaofeng Jin(金晓峰)[1,2,†]

[1] *State Key Laboratory of Surface Physics and Department of Physics, Fudan University, Shanghai* 200433, *China*
[2] *Collaborative Innovation Center of Advanced Microstructures, Fudan University, Shanghai* 200433, *China*

(Received 26 May 2016; revised manuscript received 31 May 2016; published online 25 August 2016)

The spin Hall effect has been investigated in 10-nm-thick epitaxial Au (001) single crystal films via H-pattern devices, whose minimum characteristic dimension is about 40 nm. By improving the film quality and optimizing the in-plane geometry parameters of the devices, we explicitly extract the spin Hall effect contribution from the ballistic and bypass contribution which were previously reported to be dominating the non-local voltage. Furthermore, we calculate a lower limit of the spin Hall angle of 0.08 at room temperature. Our results indicate that the giant spin Hall effect in Au thin films is dominated not by the interior defects scattering, but by the surface scattering. Besides, our results also provide an additional experimental method to determine the magnitude of spin Hall angle unambiguously.

Keywords: gold thin film, spin Hall effect, surface scattering

PACS: 72.15.–v, 85.75.–d **DOI:** 10.1088/1674-1056/25/10/107201

1. Introduction

The spin Hall effect (SHE), which exploits the interplay of charge and spin, has attracted much attention in the field of spintronics. In presence of the spin–orbit coupling, a transverse spin current, which is widely believed to be beneficial for potential applications, is generated via a charge current driven by a voltage gradient.[1,2] Therefore, from a practical application point of view, large spin Hall angle (SHA), i.e., the converting efficiency from charge current to spin current, is highly desired.[3]

The exploration for the larger SHA largely relies on the understanding of the underneath mechanisms. It is widely accepted that the SHE and the anomalous Hall effect (AHE) share the same origin,[4,5] of which three mechanisms have been proposed to account for the left–right asymmetry. Among them, the skew scattering[6] and the side jump[7] are realized upon electrons scattered by local potential created by foreign impurities or defects, known as the extrinsic mechanisms. In contrast, the intrinsic mechanism is solely determined by the electronic band structure.[8,9] Therefore, the intrinsic mechanism leaves limited choices for artificial modification, while the magnitude of extrinsic mechanism, with various combinations of impurities and hosts, can be effectively tuned.[10–12]

Furthermore, since the source of the scattering centers include foreign impurities, as well as the surface, and crystal defects,[13] it is possible that the extrinsic mechanism becomes more pronounced in thin films.[14] A recent experiment employing a H-pattern in 10-nm-thick Au indicated a large SHA of about 0.1, while a relative small SHA was reported by subjecting 60-nm-thick Au to similar measurement.[15] Besides, a previous paper also reported that the SHA of pure Au, where no impurity is intentionally doped, was strongly reduced with thickness increasing.[16] All those results appear to imply a sound logic that the surface scattering plays a crucial role at thin films, because the thinner the film, the more efficient the surface scattering.

The single crystal Au thin film, with minimum defects at the interior, manifests itself as a good platform to study the surface scattering. The physical picture is as follows: for the electrons traveling in a thin film with thickness comparable to the mean free path, the electrons should be scattered by both interior defects, and surfaces. The reduced defects indicates a longer mean free path at the interior, thereby ultimately results in the increasing of the surface scattering contribution. In an extreme case of perfect crystal structure, the electrons could only be scattered by the surface. Therefore, one may expect a comparable or even higher SHA in single crystalline Au thin film, if the surface scattering is indeed significant for the SHE as expected. In this paper, we investigate the SHE in single crystalline Au thin film through H-pattern approach, and derive an SHA of 0.08 at room temperature. This magnitude is consistent with previous experimental results obtained from poly-crystalline thin films.[16–18] Thus, our result supported that the giant SHE is independent from the concentration of interior defects, but originates from the surface scattering.

2. Experimental details

We use the H-pattern to measure the SHE. Among the copious efforts waged on the SHE investigation, the H-pattern

*Project supported by the National Basic Research Program of China (Grant Nos. 2015CB921400 and 2011CB921802) and the National Natural Science Foundation of China (Grant Nos. 11374057, 11434003, and 11421404).

†Corresponding author. E-mail: xfjin@fudan.edu.cn

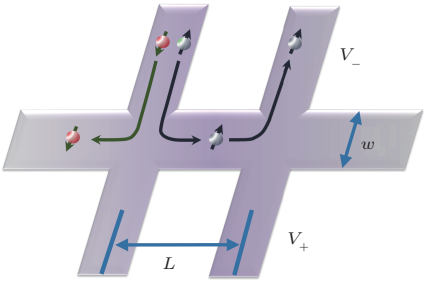
© 2016 Chinese Physical Society and IOP Publishing Ltd

approach, with the capability of employing the spin current generation and detection within one layer, avoids the complex issues originated from the spin current transporting through the interface among layers.[19–21] In principle, the H-pattern thus allows an accurate determination of the SHA without involving other mechanisms or complicated modeling.

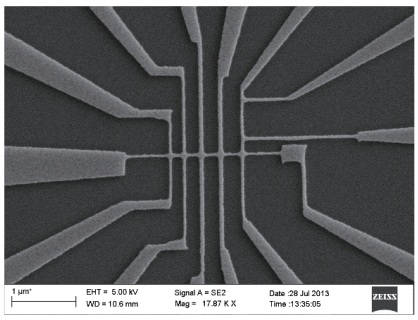
As shown in Fig. 1(a), by applying current I through the left bar, the resultant V_{nl} is measured at the right bar, thus R_{nl} defines as V_{nl}/I. One may expect a non-local resistance $R_{\rm sH}$ from SHE contribution based on quasi one-dimensional (1D) spin diffusion process:[22] [see Fig. 1(a)]

$$R_{\rm sH} = \frac{1}{2}\alpha^2 \frac{w}{l_{\rm s}} \exp\left(-\frac{L}{l_{\rm s}}\right), \tag{1}$$

where L and w refer to devices lateral geometries as explained in the caption of Fig. 1(a). α and $l_{\rm s}$ represent spin Hall angle and spin diffusion length, respectively.



(a)



(b)

Fig. 1. (color online) (a) The SHE contribution existed in H-pattern measurement as explained in the text. L stands for the center to center distance of two adjacent bars. w is the horizontal bridge width. Note that the $R_{\rm sH}$ is positive. (b) Scanning electron microscopy image of H-pattern device, with several vertical bars separated by various distance L and connected by central bridge of width $w = 40$ nm. The R_{nl} is obtained from bar distance L of 200 nm unless specifically mentioned.

However, H-pattern measurement is not without controversies and complications. Early attempts with 60-nm-thick Au films performed by Mihajlović *et al*. suggest that the resultant non-local resistance is dominated by the additional undesired diffusive charge contribution (bypass contribution) $R_{\rm c}$ and ballistic transport contributions $R_{\rm b}$ instead of SHE $R_{\rm sH}$.[15] Thus, the total $R_{nl} = R_{\rm c} + R_{\rm b} + R_{\rm sH}$. Recently, it has been demonstrated that the $R_{\rm sH}$ can be observed by enlarging device lateral geometry ($w > l_{\rm s}$) and reducing film thickness. Remarkably, the temperature dependency of the reported signal is solidly evidenced to be from $R_{\rm sH}$, and an SHA of about 0.1 is derived from 10-nm-thick poly-crystalline Au films. However, the quantitative analyses must rely on the assumption that no $R_{\rm b}$ residue is remaining, and resort to Eq. (1) which is only valid in the frame of $w < l_{\rm s}$.

We notice that the ballistic contribution $R_{\rm b}$ is a secondary effect of the bypass contribution $R_{\rm c}$ which decays exponentially with w decreasing,[5] while the SHE contribution, on the other hand, decreases linearly. In principle, with a proper combination of w and L, the $R_{\rm sH}$ should be larger than $R_{\rm c}$ and $R_{\rm b}$. In addition, the $R_{\rm sH}$ is always positive due to the underlying mechanism, while $R_{\rm c} + R_{\rm b}$ is supposed to remain negative at narrow w. Those different scaling dependencies on w could be the traces that ultimately lead to the unambiguous determination of $R_{\rm sH}$. The previous experiments preclude such investigation for the reliability of narrow w devices is hindered by the poly-crystalline nature of the film.

To this end, we here have fabricated H-pattern based on both poly and single crystalline 10-nm Au film with w ranging from 70 nm to 40 nm. Although the single crystalline nature enhances the negative ballistic contribution $R_{\rm b}$ due to the longer electron mean free path $l_{\rm e}$, it also ensures the possibility of fabrication of extremely small devices. Fortunately, the different behaviors of measured R_{nl} with various w are clearly observed and allow us to separate the $R_{\rm sH}$.

Two types of Au film have been prepared in our experiments. The poly-crystalline Au film devices have been patterned into nanometer scale H-pattern by standard lift-off process through electron-beam lithography (EBL) on SiO_2/Si substrate before the film deposition by E-beam evaporation.

The single-crystalline Au films, on the other hand, were prepared on MgO (001) substrate by molecular beam epitaxy in an ultra-high vacuum system with base pressure of 1×10^{-7} Pa, ahead of any patterning processes. Before the deposition, the MgO (001) substrate was annealed at 500 °C for 60 min in order to form a clean and plain surface. Additionally, the Au film was *in-situ* annealed at 200 °C for 30 min after the deposition. The crystal quality of annealed MgO substrate and 10-nm Au with (001) were characterized by reflection high-energy electron diffraction (RHEED) technique. Clean and sharp RHEED patterns were obtained and presented as the inset of Fig. 2(a). Once the film preparation is completed, H-pattern structures were fabricated via negative resist-based EBL and Ar ion etching method. An extraordinary narrow horizontal bridge with $w = 40$ nm is achieved. Figure 1(b) demonstrates the scanning electron microscopy image of a complete device. The electrical measurements were performed by the DC reverse technique in combination with a Keithley 2182 nanovolt meter and 2400 source meter with a bias current ranging from 100 μA to 300 μA.

3. Results and discussion

The value of resistivity ρ_{xx} is always an essential factor for assessing the film quality. The resistivity measurement of 10-nm thick Au films with different crystalline nature have been performed through 5 K to room temperature as demonstrated in Fig. 2(a). The result from both the poly-crystal and single-crystal film show common temperature dependency, i.e., the ρ_{xx} decrease linearly with temperature decreasing, as expected for normal metal films. However, their values are largely different. The ρ_{xx} in single-crystal film is $3.86\times10^{-8}\ \Omega\cdot$m at room temperature, nearly three times smaller than that in poly-crystal film of $1.19\times10^{-7}\ \Omega\cdot$m, due to the significantly improved crystal quality. Thereby a much longer l_e (3 times) should also be expected in single-crystal film.

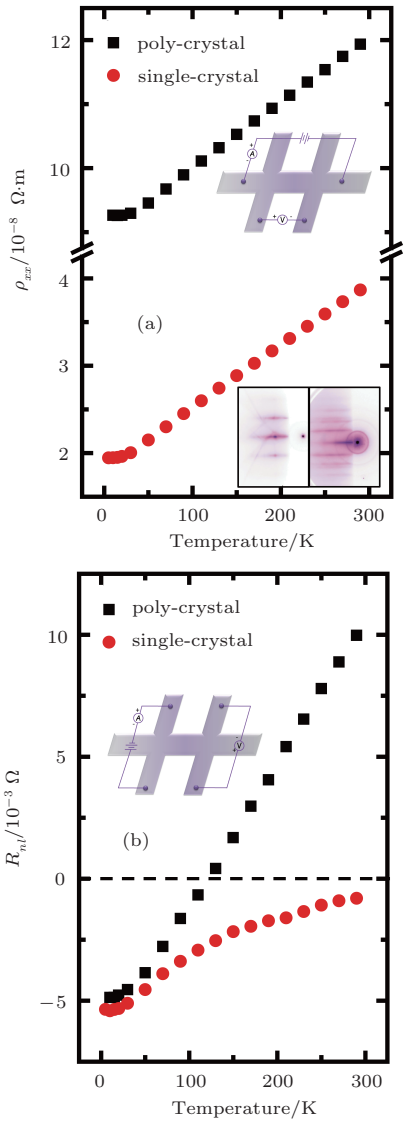


Fig. 2. (color online) (a) Resistivity ρ_{xx} of 10-nm thick poly-crystalline (black) and single-crystalline (red) Au film as a function of temperature. Upper inset: the schematic map of the 4-probe measurement configuration. Lower inset: the RHEED pattern of the annealed MgO substrate (left) and the single crystal Au film (right). (b) Temperature dependency of R_{nl} measured for devices of $w = 70$ nm with different crystal quality. Inset: schematic map of the non-local measurement.

Figure 2(b) shows the nonlocal resistance of R_{nl}, measured from both poly- and single-crystalline sample with $w =$ 70 nm from 5 K to 290 K. We employ the non-local measurement by applying current I through the left bar hence the V_+ and V_- for detection, as shown as inset of Fig. 2(b). The R_{nl}, thereby, is defined as V_{nl}/I. At room temperature, the R_{nl} for poly-crystalline sample is positive. With temperature decreasing to around 120 K, the sign of R_{nl} is reversed to negative. Such behavior has been well explained by the combination of the charge diffusive contribution R_c and electron ballistic contribution R_b that spontaneously entangles with R_{sH}. Phenomenologically one can describe the R_{nl} by[5]

$$R_c + R_b = R_c\left[1 - b\exp\left(-\frac{w}{l_e}\right)\right], \tag{2}$$

where

$$R_c = R_{sq}\exp\left(-\frac{\pi L}{w}\right) \tag{3}$$

with R_{sq} being the sheet resistance defined as film resistivity ρ_{xx} divided by thickness t. b is a dimensionless parameter, which may depend on electron rebound trajectories. l_e denotes the electron mean free path. As expected from the bypass contribution R_c, at room temperature, the l_e is relatively small compared to the bridge width w, thus $R_c + R_b > 0$. When temperature is lower, R_{nl} decreases due to the increasing l_e. As a result, the second term in Eq. (2) becomes negative and leads to a negative R_{nl} at around 120 K. As for the single crystal, the perfect crystalline indicates a longer l_e from 5 K to room temperature. Therefore, the R_{nl} remains negative within the entire temperature range.

Although the magnitude of R_{nl} in two samples are about the same scale at 5 K, it does not indicate the ballistic contributions can be equally treated. One may notice that the ρ_{xx} is utterly different between the two types of Au film, such as R_{sq}. In Fig. 3(a), we presented the R_{nl}/R_{sq} as a function of temperature. It is immediately clear that the ballistic contribution is much more significant in single-crystalline sample at 5 K, consistent with previous understanding. Besides, the negative sign of R_{nl}/R_{sq} further supports our speculation that $R_c + R_b$ is negative when w is narrow enough. Apparently, if the R_{nl} is solely consisting of $R_c + R_b$, R_{nl} should remain negative with w further reducing.

To examine the speculation, the nonlocal measurement has been carried out in single crystal devices with $w = 50$ nm and $w = 40$ nm. The temperature dependency of R_{nl} and R_{nl}/R_{sq} are shown in Figs. 3(b) and 3(c). With w reducing to 50 nm, the absolute value of the R_{nl}/R_{sq} is slightly smaller than that in $w = 70$ nm due to the reduced lateral geometry, as can be seen from Eq. (2). But the sign of R_{nl}/R_{sq} is positive at room temperature, and again reverses to negative upon temperature decreasing. Even more surprisingly, when $w = 40$ nm,

R_{nl} remains positive within the entire temperature range. In contrast, the negative R_{nl} is observed in $w = 70$ nm devices even at room temperature due to the acute ballistic contribution. Such behavior cannot be convincingly explained with previous understandings.[15]

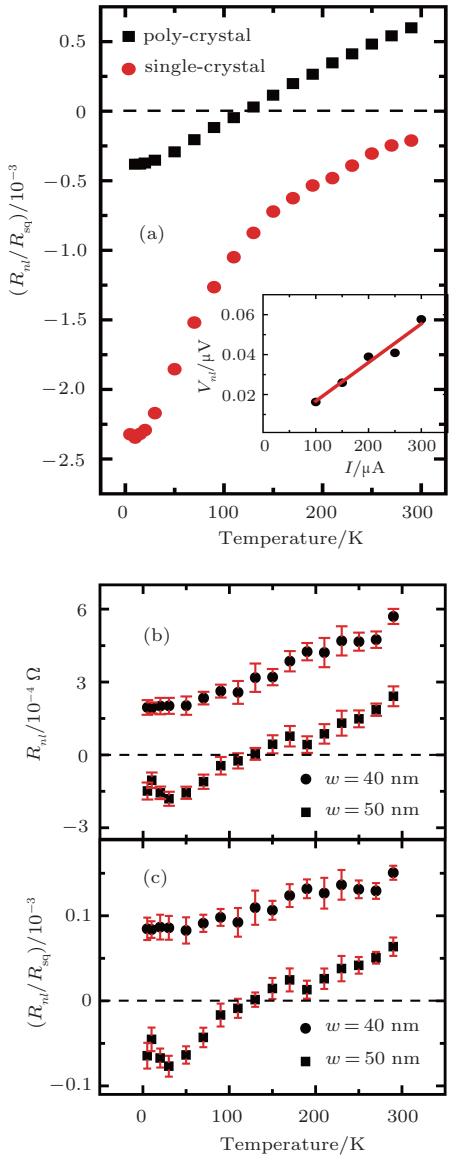


Fig. 3. (color online) (a) R_{nl}/R_{sq} as a function of temperature. Inset: I–V curve obtained form nonlocal measurement in single-crystal Au film devices with the central bridging wire $w = 40$ nm at 5 K. The linear dependency ensures the V_{nl} results from the applied current. Temperature dependency of R_{nl} (b) and R_{nl}/R_{sq} (c) for $w = 40$ nm and $w = 50$ nm.

The inset of Fig. 3(a) shows the result of bias-dependent measurement stems from $w = 40$ nm sample at 5 K. The linear dependency of the nonlocal voltage on applied current ensures the effectiveness of the data, and our DC reverse technique helps to rule out Joule heating effect or the thermoelectric effects induced thermal voltage. As described by Eq. (2) and demonstrated by R_{nl}/R_{sq} in 70 nm, $R_c + R_b$ is negative once w is narrow enough in respect to l_e. Therefore, if the R_{nl} solely consists of R_c and R_b, or R_{sH} is negligibly small, for a given device with set lateral geometry and l_e, one should expect that R_{nl} remains negative once w is below a critical value which is obviously opposite to our observations. It thus evidences that an additional positive contribution from R_{sH} must exist, and the $R_c + R_b$ is negligibly small, if at all.

Using the obtained R_{nl}/R_{sq} from $w = 40$ nm, which are 0.085×10^{-3} at 5 K and 0.15×10^{-3} at room temperature, and Eq. (1), we are able to calculate the SHA. With an l_s of 86 nm for a gold film prepared on MgO with a similar resistivity of $2.7\mu\cdot\Omega\cdot$cm,[17] we calculated the SHA of 0.08 at room temperature. We note that the value is larger than some of α in previous reports,[15,23–25] but consistent with the result reported by[16–18] based on the electrical injection experiments in poly-crystalline 10-nm-thick Au film, supporting the conclusion that the giant SHA is attributed to the surface scattering. Besides our results are also in agreement with the early determination of 8 percent polarization asymmetry in gold foil through double Mott scattering experiment.[26]

As for other combinations with L longer than 200 nm, the V_{nl} is practically zero and does not obviously respond to applied current, indicating the resultant R_{nl} is beyond the resolution of our measurement. In addition, the temperature dependency of R_{nl}/R_{sq} with $w = 40$ nm is also unexpected. Normally the magnitude of SHE-related nonlocal voltage should monotonically decay with increasing temperature due to the decreasing of l_s. But it is important to note the equation (1) varies with l_s in a non-monotonic manner. Such a behavior may be responsible for this discrepancy. Based on Eq. (1) with $w = 40$ nm and $L = 200$ nm, the R_{sH}/R_{sq} is deduced to be increasing with increasing l_s at short l_s, and reaching the maximum value at around $l_s = 160$ nm before decreasing at longer l_s.

Although one cannot derive the l_s in our sample from current results, however, given the ρ_{xx} in single crystal is 3 times smaller than that in poly-crystal at 5 K[27,28] and the l_s for a poly-crystal gold film at 10 K is 63 nm,[19,29] it is quite reasonable to expect an l_s larger than 160 nm in single-crystalline sample. If this is the case, the obtained SHA is a lower limit. Another possible reason could be the residual $R_c + R_b$. Despite the R_{sH} overruns the $R_c + R_b$ in magnitude, but the temperature dependency may be dominated by the latter. However, with $b = 20l_e = 40$ nm, $l_s = 70$ nm, $\alpha = 0.1$, the calculated R_{sH} is about 1.64×10^{-4}, orders of magnitude larger than the calculated $R_c + R_b = -9.65 \times 10^{-7}$. Thus, $R_c + R_b$ is very unlikely dominating the temperature dependency of R_{nl}. In contrast, with $w = 50$ nm, $R_c + R_b$ is calculated to be -1.66×10^{-5}, comparable with R_{sH}. Nevertheless, a significantly smaller device should bring deeper insight to this issue, but we are not able to achieve such device currently. Besides the extremely small R_{nl} probably makes it impractical to acquire a solid signal.

4. Conclusion

In conclusion, we reported a series of investigations of R_{nl} in gold H-pattern fabricated based on both poly-crystal film and single-crystal film. Our analysis shows that the positive R_{nl} in narrow w devices arises from the SHE effect. With the finite signal obtained, we acquire an SHA of 0.08 in 10-nm-thick single-crystal Au film, indicating that a giant SHE originates from the surface scattering as expected, instead of the interior defects. In addition, our results prove that a clean SHE contribution can be unambiguously detected solely by optimizing the device's geometry without resorting to external magnetic field, additional layers or complicated modeling, thus extending the boundary on the SHE investigation.

References

[1] Hirsch J E 1999 *Phys. Rev. Lett.* **83** 1834
[2] Dyakonov M I and Perel V I 1971 *Phys. Lett.* **35** 459
[3] Wolf S A, Awschalom D D, Buhrman R A, Daughton J M, Molnr S von, Roukes M L, Chtchelkanova A Y and Treger D M 2001 *Science* **294** 1488
[4] Nagaosa N, Sinova J, Onoda S, MacDonald A H and Ong N P 2010 *Rev. Mod. Phys.* **82** 1539
[5] Hoffmann A 2013 *IEEE Trans. Magn.* **49** 5172
[6] Smit J 1958 *Physica* **24** 39
[7] Berger L 1970 *Phys. Rev. B* **2** 4559
[8] Karplus R and Luttinger J M 1954 *Phys. Rev.* **95** 1154
[9] Sundaram G and Niu Q 1999 *Phys. Rev. B* **59** 14915
[10] Niimi Y, Suzuki H, Kawanishi Y, Omori Y, Valet T, Fert A and Otani Y 2014 *Phys. Rev. B* **89** 054401
[11] Gradhand M, Fedorov D V, Zahn P and Mertig I 2010 *Phys. Rev. B* **81** 245109
[12] Niimi Y, Morota M, Wei D H, Deranlot C, Basletic M, Hamzic A, Fert A and Otani Y 2011 *Phys. Rev. Lett.* **106** 126601
[13] Maekawa S 2006 *Concepts in Spin Electronic* (New York: Oxford University Press) p. 357
[14] Wang X, Xiao J, Manchon A and Maekawa S 2013 *Phys.Rev. B.* **87** 081407
[15] Mihajlović G, Pearson J E, Garcia M A, Bader S D and Hoffmann A 2009 *Phys. Rev. Lett.* **103** 166601
[16] Seki T, Sugai I, Hasegawa Y, Mitani S and Takanashi K 2010 *Solid State Commun.* **150** 496
[17] Seki T, Hasegawa Y, Mitani S, Takahashi S, Imamura H, Maekawa S, Nitta J and Takanashi K 2008 *Nat. Mater.* **7** 125
[18] Gu B, Sugai I, Ziman T, Guo G. Y, Nagaosa N, Seki T, Takanashi K and Maekawa S 2010 *Phys. Rev. Lett.* **105** 216401
[19] Ji Y, Hoffmann A, Jiang J S and Bader S D 2004 *Appl. Phys. Lett.* **85** 6218
[20] Takahashi S and Maekawa S 2003 *Phys. Rev. B.* **67** 052409
[21] Fukuma Y, Wang L, Idzuchi H and Otani Y 2010 *Appl. Phys. Lett.* **97** 012507
[22] Abanin D A, Shytov A V, Levitov L S and Halperin B I 2009 *Phys. Rev. B* **79** 035304
[23] Qu D, Huang S Y, Miao B F, Huang S X and Chien C L 2014 *Phys. Rev. B* **89** 140407
[24] Obstbaum M, Härtinger M, Bauer H, Meier T, Swientek F, Back C and Woltersdorf G 2014 *Phys. Rev. B* **89** 060407
[25] Isasa M, Villamor E, Hueso L Gradhand E, M and Casanova F 2015 *Phys. Rev. B* **91** 024402
[26] Shull C G, Chase C T and Myers F E 1943 *Phys. Rev.* **63** 29
[27] Elliott R J 1954 *Phys. Rev.* **96** 266
[28] Niimi Y, Wei D, Idzuchi H, Wakamura T, Kato T and Otani Y 2013 *Phys. Rev. Lett.* **110** 016805
[29] Pierre F, Gougam A B, Anthore A, Pothier H, Esteve D and Birge N O 2003 *Phys. Rev. B* **68** 085413